International Journal of Nanomedicine

Dovepress
open access to scientific and medical research

Open Access Full Text Article

ORIGINAL RESEARCH

Vitamin E succinate-grafted-chitosan/chitosan oligosaccharide mixed micelles loaded with C-DMSA for Hg^{2+} detection and detoxification in rat liver

This article was published in the following Dove Press journal:
International Journal of Nanomedicine

Binghui Wei[1,2]
Muye He[1,2]
Xiaoran Cai[1,2]
Xinyu Hou[1,2]
Yujie Wang[1,2]
Jiaojiao Chen[1,2]
Minbo Lan[1]
Yanzuo Chen[1,2]
Kaiyan Lou[2,3]
Feng Gao[1,2,4]

[1]Shanghai Key Laboratory of Functional Materials Chemistry, East China University of Science and Technology, Shanghai 200237, People's Republic of China; [2]Department of Pharmaceutics, School of Pharmacy, East China University of Science and Technology, Shanghai 200237, People's Republic of China; [3]State Key Laboratory of Bioengineering Reactor, Shanghai Key Laboratory of New Drug Design and Shanghai Key Laboratory of Chemical Biology, School of Pharmacy, East China University of Science & Technology, Shanghai 200237, People's Republic of China; [4]Shanghai Key Laboratory of New Drug Design, East China University of Science and Technology, Shanghai 200237, People's Republic of China

Correspondence: Feng Gao; Kaiyan Lou
East China University of Science and Technology, 130 Meilong Road, Shanghai 200237, People's Republic of China
Tel +86 21 6425 2449; +86 21 6425 3299
Fax +86 21 6425 8277
Email fgao@ecust.edu.cn; kylou@ecust.edu.cn

Aim: To determine whether the use of a mixed polymeric micelle delivery system based on vitamin E succinate (VES)-grafted-chitosan oligosaccharide (CSO)/VES-grafted-chitosan (CS) mixed micelles (VES-g-CSO/VES-g-CS MM) enhances the delivery of C-DMSA, a theranostic fluorescent probe, for Hg^{2+} detection and detoxification in vitro and in vivo.

Methods: Mixed micelles self-assembled from two polymers, VES-g-CSO and VES-g-CS, were used to load C-DMSA and afforded C-DMSA@VES-g-CSO/VES-g-CS MM for cell and in vivo applications. Fluorescence microscopy was used to assess C-DMSA cellular uptake and Hg^{2+} detection in L929 cells. C-DMSA@VES-g-CSO/VES-g-CS MM was then administered intravenously. Hg^{2+} detection was assessed by fluorescence microscopy in terms of bio-distribution while detoxification efficacy in Hg^{2+}-poisoned rat models was evaluated in terms of mercury contents in blood and in liver.

Results: The C-DMSA loaded mixed micelles, C-DMSA@VES-g-CSO/VES-g-CS MM, significantly enhanced cellular uptake and detoxification efficacy of C-DMSA in Hg^{2+} pretreated human L929 cells. Evidence from the reduction of liver coefficient, mercury contents in liver and blood, alanine transaminase and aspartate transaminase activities in Hg^{2+} poisoned SD rats treated with the mixed micelles strongly supported that the micelles were effective for Hg^{2+} detoxification in vivo. Furthermore, ex vivo fluorescence imaging experiments also supported enhanced Hg^{2+} detection in rat liver.

Conclusion: The mixed polymeric micelle delivery system could significantly enhance cell uptake and efficacy of a theranostic probe for Hg^{2+} detection and detoxification treatment in vitro and in vivo. Moreover, this nanoparticle drug delivery system could achieve targeted detection and detoxification in liver.

Keywords: micelles, C-DMSA, mercury poisoning, detection and detoxification, drug delivery system

Introduction

Mercury ion (Hg^{2+}) is a highly toxic heavy metal ion, which can cause serious health problems, such as kidney failure, central nervous system damage, abnormal liver functions and even death.[1] It has raised significant concerns as an environmental contaminant and health threat to people and wildlife. Great efforts have been made for its effective treatment and selective detection.[2–11] Hg^{2+} poisonings were mainly treated with heavy metal chelators including 2,3-dimercaptopropanol

submit your manuscript | www.dovepress.com
DovePress
http://doi.org/10.2147/IJN.S213084

(British Anti Lewisite, BAL), D-penicillamine, meso-2,3-dimercaptosuccinic acid (DMSA)[2] and 2,3-dimercaptopropanesulphonate.[3] Antioxidants such as vitamin E, glutathione and lipoic acid were used in mercury ion detoxification as well.[4,5] For example, meanwhile, many selective and sensitive techniques were developed for selective and sensitive Hg^{2+} detection, which included atomic absorption spectroscopy,[6] inductively coupled plasma mass spectrometry,[7] and fluorescent probes[8,9] and nanoparticle-based sensors.[10,11]

While most of the literature work focused only on either Hg^{2+} detection[12] or detoxification, we approached from a theranostic perspective and designed the first generation of small-molecule-based theranostic fluorescent probe C-DMSA (Figure 1) for simultaneous detection and detoxification of Hg^{2+} ion.[13] The probe undergoes Hg^{2+}-promoted hydrolysis and dithioacetal cleavage to afford coumarin-aldehyde for fluorescence turn-on response and simultaneously obtain stable DMSA-Hg^{2+} complex[14] for mercury ion detoxification (Figure 1). In the previous studies, we demonstrated that C-DMSA has excellent selectivity for Hg^{2+} detection over many other metal ions tested and the probe also exhibits low toxicities and could effectively protect MCF-7 cells against Hg^{2+}-induced cell toxicity in methyl thiazolyl tetrazolium (MTT) assays.[13] However, the probe suffered from poor cell penetration and could not detect Hg^{2+} inside cells.[13] Moreover, the in vivo efficacy of C-DMSA in Hg^{2+} detection and detoxification has not been explored. To address these issues, we envisioned to use a nanoparticle-based drug delivery system to enhance cellular uptake of C-DMSA and to explore its potentials in in vivo Hg^{2+} detection and detoxification. In particular, we could take advantage of size-dependent non-specific uptake of nanoparticles with sizes lower than 200 nm to achieve liver-targeting ability,[14] and to investigate the Hg^{2+} detection and detoxification behavior of C-DMSA in liver where mercury ions tend to accumulate.[4,15]

In this study, mixed micelles[16] were prepared from two biocompatible and biodegradable polymers, vitamin E succinate-grafted-chitosan oligosaccharide (VES-g-CSO)[17] and vitamin E succinate-grafted-chitosan (VES-g-CS).[18] They were characterized and studied as the drug delivery system to enhance cellular uptake of C-DMSA and to achieve liver-targeting ability with advantages that their sizes and physicochemical properties can be conveniently tuned by changing weight ratio of the two polymers in preparation.[19,20] Further, in vitro and in vivo detection and detoxification studies of C-DMSA loaded VES-g-CSO/VES-g-CS mixed micelles were performed in cell and rat models to study the efficacy of the nano drug delivery system to enhance C-DMSA delivery inside cells and into livers in vivo.

Materials and methods

Materials

The theranostic Hg^{2+} fluorescent probe, 3-formyl-7-diethylamino coumarin masked meso-dimercaptosuccinic acid (C-DMSA), was synthesized according to the literature procedures.[11] Chitosan (CS, Mw 50 kDa, 90.0% deacetylation degree) was purchased from JinQiao Biochemical Co. Ltd. (Shandong, China). Chitosan oligosaccharide (CSO, MW 5 kDa, 90.0% deacetylation degree) was obtained from JinQiao Biochemical Co. Ltd. (Shandong, People'sRepublic of China). Vitamin E succinate (VES) was purchased from TCI Development Co. Ltd. (Shanghai, People's Republic of China). *N*-Hydroxysuccinimide (NHS) and 1-Hydroxybenzotriazole (HOBt) were purchased from Adamas Co. Ltd. Mercury perchlorate trihydrate was purchased from XianDing Biotechnology Co. Ltd. (Shanghai, People's Republic of China). All the other analytical chemicals and reagents were analytical grade. FBS, PBS, 0.25% (w/v) trypsin solution, penicillin-streptomycin and DMEM were purchased from Gibco BRL (Gaithersburg, MD, USA). IR-775 chloride, pentobarbital sodium and MTT were purchased from

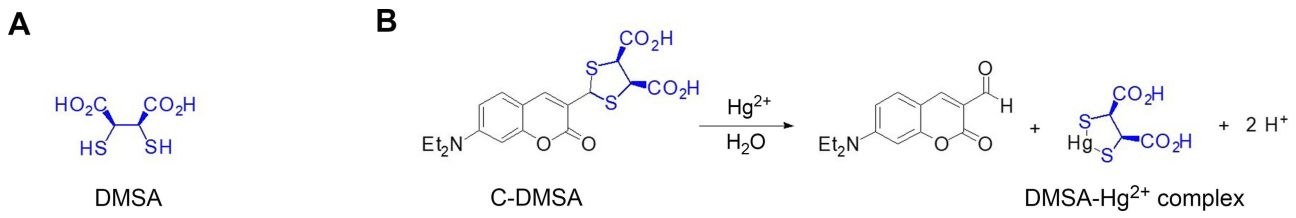

Figure 1 Structure of DMSA (**A**) and design of fluorescent theranostic agents for Hg^{2+} (**B**).
Abbreviations: DMSA, meso-2,3-dimercaptosuccinic acid; C-DMSA, 3-formyl-7-diethylamino coumarin masked meso-dimercaptosuccinic acid.

Sigma (St. Louis, USA). Hoechst 33258 was purchased from Beyotime Institute of Biotechnology (Shanghai, People's Republic of China).

Synthesis of VES-g-CSO

VES-g-CSO was synthesized via coupling of the activated carboxyl group of VES molecules with the amine groups of CSO in the presence of EDC and NHS according to our previously reported procedures.[17] CSO (500 mg) was dissolved in 25 mL of water at room temperature. VES (160 mg), EDC·HCL (156 mg) and NHS (90 mg) were dissolved in 15 mL of anhydrous ethanol and then added into the CSO solution dropwise on a magnetic stirrer, followed by stirring in the dark for 24 hrs at 25°C. The resulting solution was concentrated in vacuum and then precipitated in cold anhydrous diethyl ether. The product was collected, washed with anhydrous ethanol three times and dried under a vacuum dryer (40°C) overnight to obtain the product.[21]

Synthesis of VES-g-CS

VES-g-CS was synthesized according to the literature procedures with minor modifications.[21,22] In brief, chitosan (600 mg) and HOBt (514 mg) was dissolved in 60 mL of water and the resulting solution was stirred for 24 hrs at room temperature. VES (178 mg) was dissolved in 40 mL absolute ethyl alcohol, followed by the addition of EDC (100 mg). The resulting solution was then slowly added to the CS-HOBt solution and stirred in the dark for 24 hrs at room temperature. Then, the product was dialyzed in distilled water using a dialysis membrane (MW 1 kDa, Green Bird Inc. Shanghai, People's Republic of China) to remove hydrophilic byproducts, followed by freeze drying.

Characterization of VES-g-CS

Samples were analyzed by Fourier transform infrared (FT-IR) spectroscopy, elemental analysis and proton nuclear magnetic resonance (^{1}H-NMR) spectroscopy. FT-IR spectra of CS, VES and VES-g-CS were recorded in KBr pellets with a FT-IR spectrophotometer (Nicolet 6700, Thermo Fisher Scientific, Waltham, MA, USA). For ^{1}H-NMR analysis, VES-g-CS was dissolved in D_2O at 25°C and analyzed by 400 MHz NMR spectrometer (Bruker, Karlsruhe, Germany). The substitution degrees of VES to VES-g-CS were calculated based on elemental analysis performed on an element analyzer (CS-344 carbon/sulfur analyzer, LECO, St. Joseph, MI, USA).

Preparations of C-DMSA@VES-g-CSO/VES-g-CS MM

Critical micelle concentrations (CMC) of the VES-g-CSO, VES-g-CS, VES-g-CSO/VES-g-CS (w/w=8:2) were determined[23] and the micelles were prepared by self-assembly in water. For VES-g-CSO micelles, 200 μL of methanol was added to the VES-g-CSO aqueous solution (4 mg VES-g-CSO dissolved in 4 mL distilled water) and the mixed solution was sonicated with a probe-type Sonicator (BILON92-II DL, People'sRepublic of China) for 5 mins at 100 W with the pulse turned off for 1 s at intervals of 1 s. After that, the solution was stirred on a magnetic plate at 100 rpm for 2 hrs to evaporate methanol. The micelles solution was centrifuged to remove the supernatant and then re-dissolved in water for experimental use. The method for the preparation of VES-g-CS and VES-g-CSO/VES-g-CS MM was the same except that different ratios of VES-g-CSO and VES-g-CS were used.

For the preparation of C-DMSA@VES-g-CSO/VES-g-CS MM, the mixture of VES-g-CSO and VES-g-CS with a total weight of 4 mg was dissolved in 4 mL of distilled water, followed by the addition of 0.2 mL of C-DMSA methanol solution (2 mg/mL). Other steps were the same as the preparation of the VES-g-CSO/VES-g-CS MM. C-DMSA@VES-g-CSO micelles and C-DMSA@VES-g-CS micelles were similarly prepared as the C-DMSA@VES-g-CSO/VES-g-CS MM.

Characterization of the micelles

The average particle size and zeta potential of C-DMSA@VES-g-CSO/VES-g-CS MM in suspension were determined by laser diffraction using Zetasizer Nano ZS90 (Malvern Instruments, Malvern, UK) dynamic light scattering (DLS) instrument. The morphology of the micelles was examined by transmission electron microscopy (TEM) (JEM-2100, Tokyo, Japan).

C-DMSA loading efficiency (LE) and entrapment efficiency (EE)

The LE and EE of micelles for C-DMSA were calculated with the following Equations (1) and (2), respectively. The weight of C-DMSA in the micelles was calculated by subtraction of the weight of unbounded C-DMSA in the supernatant from the weight of C-DMSA added in preparation of the micelles. The amount of unbounded C-DMSA was quantified by an UV-vis spectrometer

(Thermo Scientific, Evolution 220, MA, USA) at a wavelength of 403 nm.

$$LE(\%) = \frac{\text{weight of C} - \text{DMSA in micelles}}{\text{weight of the feeding micelles and C} - \text{DMSA}} \times 100\% \quad (1)$$

$$EE(\%) = \frac{\text{weight of C} - \text{DMSA in micelles}}{\text{weight of the feeding C} - \text{DMSA}} \times 100\% \quad (2)$$

Drug release and stability profile

In vitro C-DMSA release profiles of the three micelles (C-DMSA@VES-g-CSO/VES-g-CS MM, C-DMSA@VES-g-CSO micelles and C-DMSA@VES-g-CS micelles) were studied in PBS buffer containing 0.5% (w/w) tween-80 media. The micelles solution (1 mL, 1 mg/mL micelles) was first placed in a dialysis bag (MW 1 kDa, Green Bird Inc. Shanghai, People'sRepublic of China). The dialysis bag was then submerged in 19 mL of PBS buffer and stirred at 100 rpm at room temperature. At time points of 0.08, 0.25, 0.5, 1, 2, 4, 8, 12, 24, 48 and 72 hrs, 1 mL dialysis solution sample was taken out and an equal volume of fresh medium was added. The amount of C-DMSA released in the dialysis solution at different time points were quantified by the UV-vis spectrometer at 403 nm.

For stability studies, micelles were stored at 4°C and particle sizes were measured on the day 0, 2, 4, 6, 8, 10, 12 and 14.

Cell culture

The L929 cell line was purchased from Stem Cell Bank, Chinese Academy of Sciences (Shanghai, People's Republic of China). The cells were cultured in DMEM medium containing 10% (v/v) FBS and 1% penicillin-streptomycin. The cells were maintained in a humidified incubator at 37°C with 5% CO_2 and precultured until a confluence of 80–90% was reached before the experiment.

Cell uptake

L929 cells were seeded at a density of 1×10^5 cells/mL in a 6-well plate and incubated for 24 hrs. Subsequently, culture medium from each well was replaced with the C-DMSA containing medium (C-DMSA@VES-g-CSO/VES-g-CS MM containing 20 μg/mL of C-DMSA or 20 μg/mL free C-DMSA) or same volume of saline and cells were incubated for 4 hrs. After that, 5 μL Hoechst 33258 was added to each well and cells were incubated for additional 15 mins. Finally, cells were washed with PBS and then observed with Ti-S fluorescence microscope (Nikon, Japan).

For flow cytometry (BD, San Jose, USA) studies, L929 cells were seeded and cultured similarly, except that Hoechst 33258 was not added.

In vitro fluorescence detection of Hg^{2+}

L929 cells were seeded in 24-well plates at cell density of 5×10^4 cells/well and incubated for 24 hrs. 200 μL of RPMI-1640 solution containing Hg^{2+} (4 μg/mL) was added into each well and incubated for 1 hr. The free C-DMSA (20 μg/mL) and C-DMSA@VES-g-CSO/VES-g-CS MM (containing 20 μg/mL C-DMSA) were then added. After incubation for additional 4 hrs in the dark, cells were observed with fluorescence microscope.[24,25]

In vitro Hg^{2+} detoxification studies

In vitro detoxification efficacy of C-DMSA@VES-g-CSO/VES-g-CS MM and C-DMSA to Hg^{2+} poisoning was tested on L929 cells by MTT assay. Cells were seeded at a density of 1×10^4 cells/well in a 96-well plate. After incubation for 24 hrs, the growth medium was replaced with 200 μL of RPMI-1640 solution containing Hg^{2+} (4 μg/mL). 200 μL of medium containing different concentrations of free C-DMSA (0.1–10 μg/mL) or C-DMSA@VES-g-CSO/VES-g-CS MM (containing 0.1–10 μg/mL C-DMSA) was then added to separate wells. After incubation for 24 hrs in the dark, the incubation medium was replaced with fresh medium.[26,27] 5 mg/mL MTT solution (200 μL/well) was added with incubation for 4 hrs. The supernatant was removed, dimethyl sulfoxide (200 μL/well) was added, and the samples were shaken for 10 mins. The absorbance of each well was measured at 570 nm by a microplate reader (Tecan Safire2, Männedorf, Switzerland).

Bio-distribution studies

Male BABL/c mice and SD rats were purchased from SLAC Laboratory Animal Co. Ltd. (Shanghai, People's Republic of China). All animals were cared for in accordance with the guidelines of the National Institute of Health for laboratory use and housed in groups as per study protocol under 12 hrs light and dark cycles and fed with a normal diet and water ad libitum. Before experiments, all animals were acclimatized for 2 weeks. The experiments were conducted in accordance with the UK Animals (Scientific Procedures) Act, 1986 and associated

guidelines, EU Directive 2010/63/EU for animal experiments. The animals were also treated according to the protocols evaluated and approved by the Ethical Committee of the East China University of Science and Technology.

IR-775, a near-infrared fluorescent dye,[28] was loaded to the mixed micelles similar to afford IR-775@VES-g-CSO/VES-g-CS MM for facile tracing locations of the mixed micelles. The bio-distribution of micelles in mice was determined after tail intravenous injection of IR-775@VES-g-CSO/VES-g-CS MM (100 μL, containing 50 μg/mL IR-775) and compared with that of IR-775 (100 μL, containing 50 μg/mL IR-775) injection. Briefly, four mice were randomly grouped into two groups (n=2 mice/group) and anesthetized by intraperitoneal injection of 0.15 mL phenobarbitone (10 mg/mL). The anesthetized mice in the same group were given free IR-775 or IR-775@VES-g-CSO/VES-g-CS MM. Mice were euthanized at 2-hr post-treatment, and different organs (heart, lung, liver, kidney and spleen) were harvested.[29] The organs were gently washed and then fluorescent photographs were taken under fluorescent spectral imager (Jitian Inc., Beijing, People's Republic of China). The excitation wavelength and emission wavelength are 770 and 810 nm, respectively, with an exposure time of 10 mins.

C-DMSA loaded mixed micelles for Hg^{2+} detection in poisoned mice

Eighteen mice were randomly divided into six groups (n=3 mice/group). The mice in control group were treated with 0.2 mL saline via intraperitoneal injection, and after 24 hrs, additional 0.2 mL saline was injected via tail vein. The second group of mice was also treated with 0.2 mL saline via intraperitoneal injection, and after 24 hrs, 0.1 mg/kg of the C-DMSA loaded mixed micelles in 0.2 mL saline was injected via tail vein. The remaining groups of mice were first treated with $HgCl_2$ at the dosage of 6 mg/kg via intraperitoneal injection, and then 24 hrs after injection, 0.2 mL saline, free C-DMSA (0.1 mg/kg) in 0.2 mL saline, C-DMSA@VES-g-CSO/VES-g-CS MM (0.1or 0.2 mg/kg) in 0.2 mL saline was injected via tail vein, respectively. Mice were euthanized 2-hr post-treatment, and different organs (heart, lung, liver, kidney and spleen) were dissected. The organs were gently washed and fluorescent photographs were taken under fluorescent spectral imager (Jitian Inc.). The excitation wavelength and emission wavelength were 477and 503 nm, respectively, with an exposure time of 3 mins.

C-DMSA loaded mixed micelles for Hg^{2+} detoxification in poisoned rats

Detoxification effects of C-DMSA@VES-g-CSO/VES-g-CS MM were evaluated in SD rats, which weighed from 170 to 190 g and were fed on a standard rat chow. Thirty rats were randomly divided into five groups (n=6 rats/group). For control group, rats were administered with 0.5 mL 0.9% saline solution via intraperitoneal injection. Rats in the other four poisoned groups were treated with 3 mg/kg $HgCl_2$ in 0.5 mL 0.9% saline via intraperitoneal injection. After 30 mins, for the control group and one poisoned group, the rats were injected with 0.5 mL saline. Another group of poisoned rats were injected with 15 mg/kg of C-DMSA in 0.5 mL 0.9% saline via tail vein, and the remaining two groups of poisoned rats were injected with C-DMSA@VES-g-CSO/VES-g-CS MM (15 or 30 mg/kg C-DMSA) in 0.5 mL saline, respectively. Forty-eight hours after the injection of $HgCl_2$, all rats were sacrificed, and samples of blood and liver were collected for analysis of Hg^{2+} content and liver functions.[15,30] Moreover, alanine transaminase (ALT) and aspartate transaminase (AST) activities in blood were also measured as biomarkers for evaluation of liver functions. Besides, liver coefficients were calculated with the following Equation (3) as an additional detoxification index.

$$\text{Liver coefficient}\% = \frac{\text{weight of wet liver}}{\text{weight of the animal}} \times 100\% \quad (3)$$

Hg^{2+} quantification in blood and liver samples

Quantification of Hg^{2+} in blood and liver samples of SD rats were performed by atomic fluorescence spectrophotometry (AFS) after microwave digestion followed literature reported procedures with minor modifications.[31–34] Blood samples were collected in centrifuge tubes with lithium heparin anticoagulant. Dissected liver was weighed and rinsed with deionized water. Both blood and liver samples were subjected to microwave digestion (Ethos-TC, Milestone, Italy).[34,35] For microwave digestion, 0.1 g sample was entirely soaked in acidic media consisting of 2 mL of 65% w/w high purity HNO_3 (JT Baker, USA), 0.5 mL H_2O_2 (30%, w/w) and 3 mL of distilled water for 10 mins. And samples were irradiated with 800 W power of

microwave, and the digestion temperature increased to 120°C for 10 mins, and further increased to 150°C for 15 mins and then increased and maintained at 180°C for 15 mins. Finally, 4.5 mL of 0.5 g/mL potassium dichromate solution (diluted in 5% HNO_3) was added for further AFS detection on an AFS 9130 atomic fluorescence spectrophotometer (Jitian Inc.). The Hg^{2+} contents in blood and liver samples of SD rats were expressed as micrograms per gram of wet tissue weight (μg/g) for liver and micrograms per liter for blood (μg/L), respectively.

Data analysis

Data are expressed as means±standard deviations. Multiple comparisons were made with one-way analysis of variance with least significant difference using statistical software (SPSS Inc., Chicago, IL, USA). *p*-values <0.05 were considered statistically significant.

Results and discussion

Synthesis and characterization of VES-g-CS

VES-g-CS was synthesized (Figure 2A) in 74.6% yield and characterized by ^{1}H-NMR (Figure 2B), FT-IR (Figure 2C) spectra and elemental analysis. The ^{1}H-NMR spectrum showed both characteristic peaks of VES and CS (Figure S1), while the enhanced peak at 1564 cm^{-1} in IR spectrum of VES-g-CS indicated formation of amide bonds between the VES carboxylic acid groups and the free amine groups on the CS.[36] The degrees of VES substitution calculated from elemental analysis was 3.0±0.8% (Table S1). VES-g-CSO was synthesized and characterized according to our previously reported procedures.[17]

CMC of VES-g-CSO, VES-g-CS and VES-g-CSO/VES-g-CS

Micelles with different ratio of two polymers were prepared. After initial screening (data not shown), three micelles prepared from VES-g-CSO, VES-g-CS and VES-g-CSO/VES-g-CS (w/w=8:2), respectively, were selected as representative micelles/mixed micelles for C-DMSA loading and delivery studies. The corresponding CMC values of VES-g-CSO, VES-g-CS and VES-g-CSO/VES-g-CS (w/w=8:2) were determined as 61.5, 17.6 and 21.6 μg/mL in PBS (pH=7.4), respectively (Figure S2), indicating they all readily form micelles in aqueous solution.[37,38]

Preparation and characterization of C-DMSA loaded micelles

C-DMSA loaded micelles were prepared and their physicochemical properties including LE, EE, particle size, zeta potential and PI were characterized and summarized in Table 1. C-DMSA@VES-g-CSO/VES-g-CS MM showed

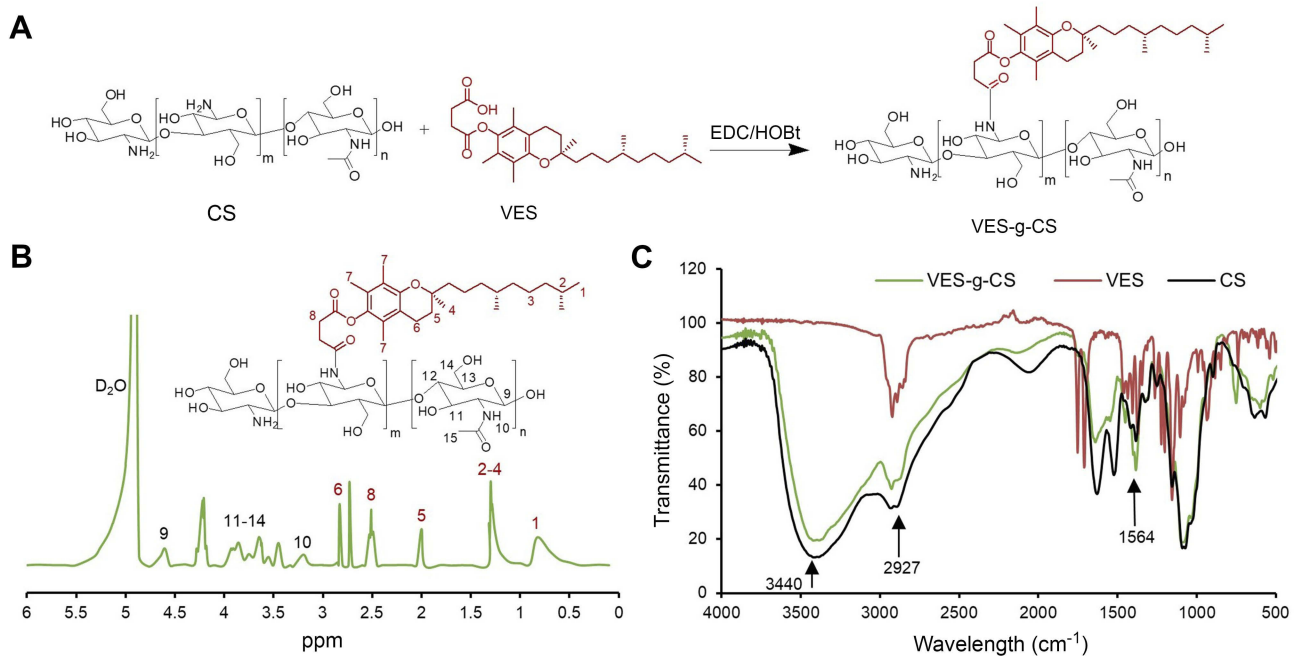

Figure 2 Synthesis of VES-g-CS (**A**), ^{1}H-NMR (**B**) and FT-IR (**C**) of VES-g-CS.
Abbreviations: VES, vitamin E succinate; CS, chitosan; VES-g-CS, vitamin E succinate-grafted-chitosan; FT-IR, Fourier transform infrared; HOBt, 1-Hydroxybenzotriazole.

Table 1 Physicochemical properties of C-DMSA loaded micelles

Micelles	LE (%)	EE (%)	Particle size (nm)	Zeta potential (mV)	PI
VES-g-CSO micelles	/	/	178.5±2.1	35.7±3.2	0.28
C-DMSA@VES-g-CSO micelles	7.5±0.2	82.8±1.5	185.3±6.2	30.9±1.9	0.21
VES-g-CS micelles	/	/	116.9±1.1	17.3±1.7	0.17
C-DMSA@VES-g-CS micelles	3.1±0.2	34.9±1.2	120.9±3.1	17.3±0.4	0.17
VES-g-CSO/VES-g-CS MM	/	/	124.5±3.5	25.6±0.9	0.16
C-DMSA@VES-g-CSO/VES-g-CS MM	6.9±0.3	76.6±1.7	133.2±4.9	24.1±0.1	0.16

Notes: Data were presented as mean±SD (n=3). "/"means the data is indeterminable.

Abbreviations: LE, loading efficiency; EE, entrapment efficiency; PI, polydispersity index; VES-g-CSO micelles, vitamin E succinate-grafted-chitosan oligosaccharide micelles; VES-g-CS micelles, vitamin E succinate-grafted-chitosan micelles; VES-g-CSO/VES-g-CS MM, vitamin E succinate-grafted-chitosan oligosaccharide/vitamin E succinate-grafted-chitosan mixed micelles; C-DMSA, 3-formyl-7-diethylamino coumarin masked meso-dimercaptosuccinic acid.

spherical morphology with an average diameter around 100 nm in a TEM image (Figure 3A) which was slightly smaller than the size in DLS (Figure 3B). This disparity was likely related to their different measurement conditions, as the TEM image was taken under dry and high vacuum condition, while DLS measurement was performed in aqueous solution.[14]

Among the three C-DMSA loaded micelles, the mixed micelles C-DMSA@VES-g-CSO/VES-g-CS MM prepared from VES-g-CSO/VES-g-CS (w/w=8:2) showed the

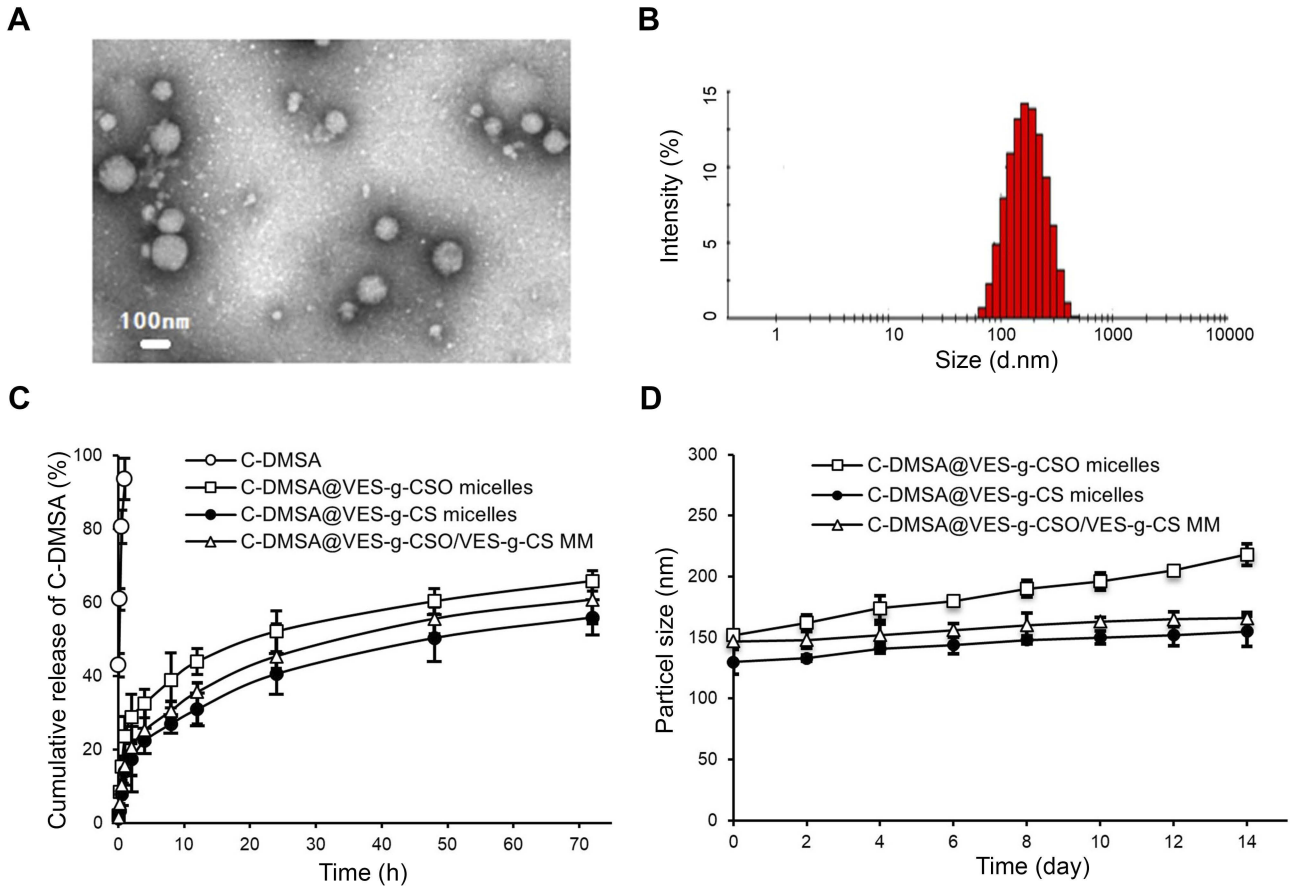

Figure 3 Transmission electron microscopy of C-DMSA@VES-g-CSO/VES-g-CS MM (**A**); particle size distribution of C-DMSA@VES-g-CSO/VES-g-CS MM obtained from dynamic light scattering (**B**); C-DMSA release profile from micelles in PBS solution (pH=7.4) (**C**) and particle size changes of C-DMSA loaded micelles stored at 4°C as a function of storage time (**D**).

Note: Data were presented as mean±SD (n=3).

Abbreviations: C-DMSA, 3-formyl-7-diethylamino coumarin masked meso-dimercaptosuccinic acid; C-DMSA@VES-g-CSO micelles, C-DMSA loaded vitamin E succinate-grafted-chitosan oligosaccharide micelles; C-DMSA@VES-g-CS micelles, C-DMSA loaded vitamin E succinate-grafted-chitosan micelles; C-DMSA@VES-g-CSO/VES-g-CS MM, C-DMSA loaded vitamin E succinate-grafted-chitosan oligosaccharide/vitamin E succinate-grafted-chitosan mixed micelles.

narrowest size distribution (PI=0.16). In addition, both C-DMSA@VES-g-CSO micelles and the mixed micelles had much higher LE and EE values than those of C-DMSA@VES-g-CS micelles indicating they were more effective in loading C-DMSA (Table 1).

In vitro drug release profiles and stability studies

The C-DMSA release profiles and stability studies of the three C-DMSA loaded micelles were performed in PBS buffer. All three micelles showed typical diffusion-based drug release profiles characterized by an initial burst release period followed by a decreasing drug release rate later (Figure 3C). Moreover, it seemed that micelles with larger sizes were associated with a faster initial C-DMSA release. Furthermore, results showed that C-DMSA@VES-g-CSO/VES-g-CS MM had the best stability in PBS buffer with no obvious size changes up to 14 days (Figure 3D).

Considering overall properties including their average particle size, PI, stability, LE and EE values, C-DMSA@VES-g-CSO/VES-g-CS MM (w/w=8:2) were selected for further in vitro and in vivo studies.

In vitro cytotoxicity study and cellular uptake

In vitro cytotoxicity of VES-g-CSO/VES-g-CS MM, C-DMSA and C-DMSA@VES-g-CSO/VES-g-CS MM were evaluated by MTT assays on a model cell line, L929 fibroblast cells. The results showed that C-DMSA loaded mixed micelles and the unloaded mixed micelles both showed low cytotoxicity up to 1.0 mg/mL (Figure S3A). Moreover, when compared with C-DMSA, C-DMSA loaded mixed micelles resulted in reduced cytotoxicity at the same concentrations (Figure S3B). Such reduced cytotoxicity is important for Hg^{2+} detoxification treatment as more C-DMSA could be tolerated as the formulation of mixed micelles.

Cellular uptakes of C-DMSA@VES-g-CSO/VES-g-CS MM were confirmed by both fluorescence microscopy and flow cytometry. When L929 cells were co-incubated with the C-DMSA loaded mixed micelles and the dye Hoechst 33258, co-staining of the green and blue fluorescence from C-DMSA and Hoechst 33258, respectively, was observed, indicating the successful cellular uptake of C-DMSA@VES-g-CSO/VES-g-CS MM (Figure 4A). Additional evidence came from flow cytometry (Figure 4B). L929 cells treated with C-DMSA@VES-g-CSO/VES-g-CS MM afforded cells with stronger fluorescence than those incubated with free C-DMSA. It was evident that the mixed micelles, with their suitable size and positive surface charge, could facilitate C-DMSA endocytosis and significantly increase intracellular C-DMSA levels.[14,22,39,40]

In vitro fluorescence detection of Hg^{2+}

Since mixed micelles could significantly increase intracellular C-DMSA levels from cell imaging studies, they would be expected to enhance Hg^{2+} detection inside cells. Indeed, when Hg^{2+}-pretreated L929 cells were incubated with C-DMSA@VES-g-CSO/VES-g-CS MM, significantly enhanced fluorescence "turn-on" response was observed compared with cells incubated with the free C-DMSA (Figure 5A), indicating improved intracellular Hg^{2+} detection by C-DMSA loaded mixed micelles.

In vitro Hg^{2+} detoxification studies

L929 cells pretreated with 2 μg/mL of Hg^{2+} for 2 hrs resulted in cell viability of 58.1±3.7% after 24 hrs

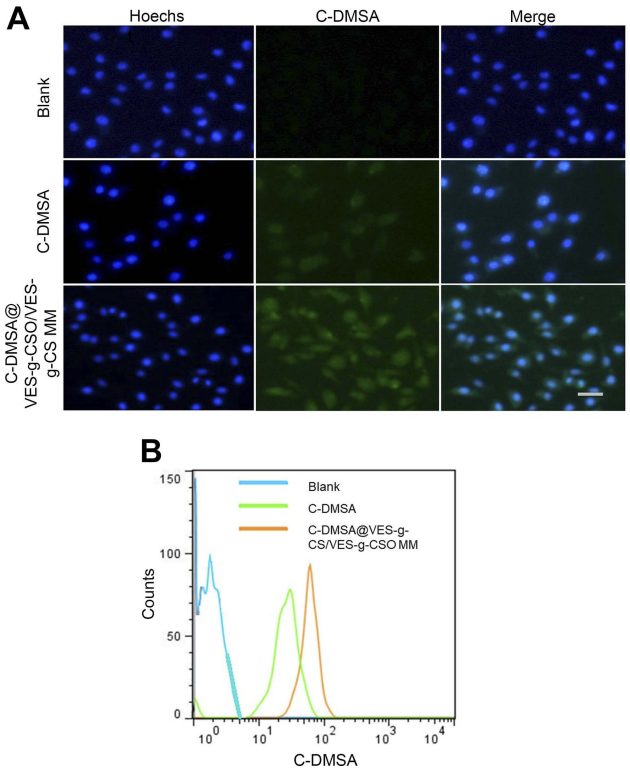

Figure 4 Fluorescence microscopy images (**A**) and flow cytometry (**B**) of L929 cells after incubation with PBS.

Notes: Blue, cell nuclei stained with Hoechst 33258; green, fluorescence of coumarin-aldehyde generated by C-DMSA after its reaction with Hg^{2+}.

Abbreviations: C-DMSA, 3-formyl-7-diethylamino coumarin masked meso-dimercaptosuccinic acid; C-DMSA@VES-g-CSO/VES-g-CS MM, C-DMSA loaded vitamin E succinate-grafted-chitosan oligosaccharide/vitamin E succinate-grafted-chitosan mixed micelles.

incubation without C-DMSA treatment. Improved cell viabilities were observed in the C-DMSA and C-DMSA@VES-g-CSO/VES-g-CS MM (0.1–10.0 μg/mL) treated cells in a concentration-dependent manner (Figure 5B), indicating that C-DMSA and the C-DMSA loaded mixed micelles could effectively protect cells from Hg^{2+}-induced cytotoxicity. Compared to free C-DMSA, C-DMSA loaded mixed micelles gave better cell survival rates at all concentrations, indicating the C-DMSA loaded mixed micelles were more effective in detoxification in cell experiments.

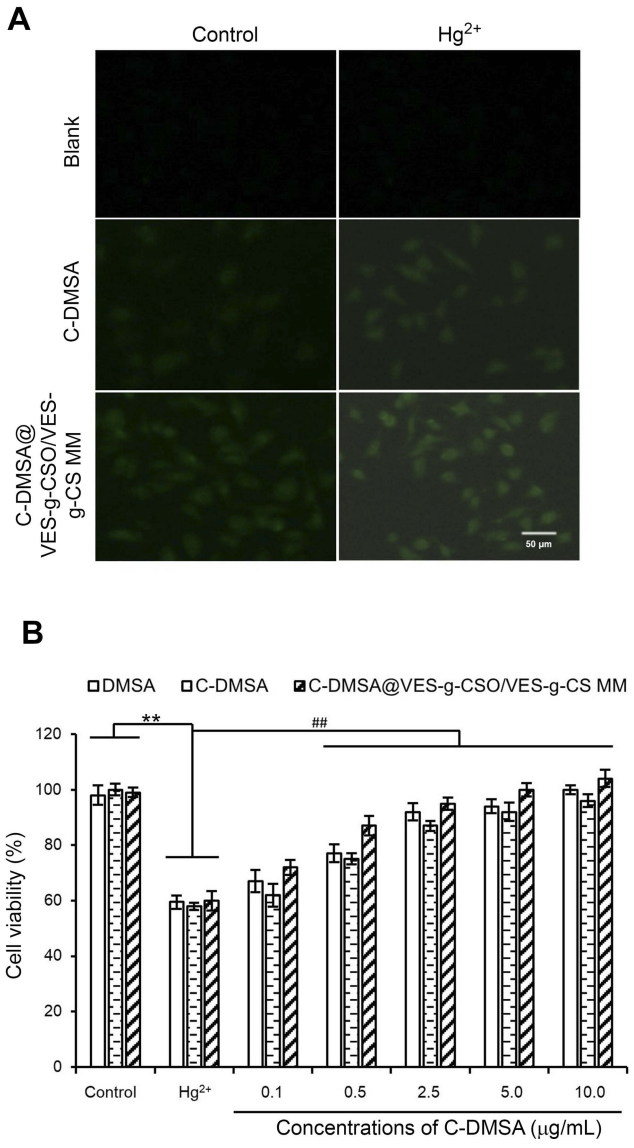

Figure 5 Fluorescence imaging intracellular Hg^{2+} of L929 cells with free C-DMSA or C-DMSA loaded mixed micelles (**A**); cell viability of L929 cells treated with Hg^{2+} and different treatments with untreated cells and poisoning group served as controls (**B**).

Notes: Left column, cells without Hg^{2+} pretreatment; right column, cells with Hg^{2+} pretreatment; top row, cells treated with PBS (blank); middle row, cell treated with C-DMSA (20 μg/mL); bottom row, cells treated with C-DMSA@VES-g-CSO/VES-g-CS MM. **p<0.01, compared to control group; ##p<0.01, compared to poisoning group. Data were presented as mean±SD (n=6).

Abbreviations: DMSA, meso-2,3-dimercaptosuccinic acid; C-DMSA; 3-formyl-7-diethylamino coumarin masked meso-dimercaptosuccinic acid; C-DMSA@VES-g-CSO/VES-g-CS MM, C-DMSA loaded micelles, vitamin E succinate-grafted-chitosan oligosaccharide/vitamin E succinate-grafted-chitosan mixed micelles.

Bio-distributions of the mixed micelles

As shown in Figure S4 and Table S2, pharmacokinetic parameters including the half-life, $AUC_{0–24\ hrs}$ and clearance (CL) of C-DMSA@VES-g-CSO/VES-g-CS MM were remarkably improved. On this basis, bio-distributions of the mixed micelles were studied by ex vivo fluorescence imaging of dissected organs (heart, lung, liver, kidney and spleen) of mice 2 hrs after intravenous injection of the IR-775 dye loaded mixed micelles via their tail vein. Significantly higher amount of IR-775 fluorescence were observed in liver compared with any other organs, while direct injection of IR-775 dye did not show any organ-specific distributions (Figure 6A). The results suggested that the mixed micelles with the size lower than 200 nm and positive charge may accumulate readily in liver via non-specific uptake mechanisms,[41] which was attributed to the uptake by reticuloendothelial system.[14,42]

Hg^{2+} detection in poisoned rats

We further tested the potential use of C-DMSA@VES-g-CSO/VES-g-CS MM in the detection of Hg^{2+} in animal models. Ex vivo fluorescence imaging studies of dissected organs were performed, as non-invasive fluorescence imaging is not possible for C-DMSA for its short fluorescence excitation/emission wavelength. Fluorescence photograph of five major organs from mice with different treatment protocols were taken and compared (Figure 6B). For the rat treated with C-DMSA loaded mixed micelles only (column c in Figure 6B), low fluorescence was observed for all dissected organs, similar with the saline control and the Hg^{2+} -poisoned rats (columns a and b in Figure 6B, respectively), as the loaded C-DMSA molecules are non-fluorescent under the imaging condition (λ_{ex}=477 nm). In contrast, when poisoned rats treated with the C-DMSA loaded mixed micelles by tail vein injection, dose-dependent high fluorescence intensities were observed 2 hrs later in liver (columns e and f in Figure 6B), indicating that micelles were targeted to liver and the loaded C-DMSA molecules reacted with Hg^{2+} to generate fluorescent product responsible for the observed fluorescence increase. Moderate fluorescence intensity increase was also observed for kidneys (columns e and f in Figure 6B), suggesting partial clearance and reaction of C-DMSA

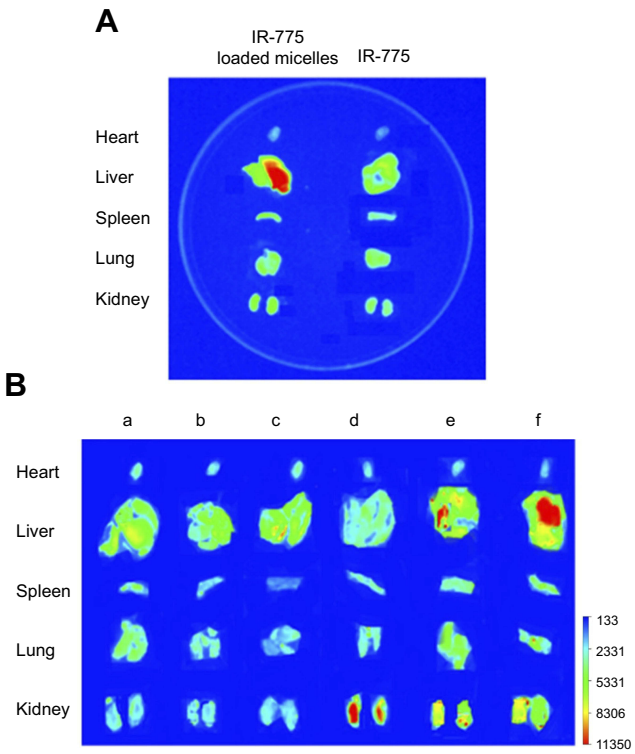

Figure 6 Ex vivo fluorescent photograph of major organs dissected from IR-775@VES-g-CSO/VES-g-CS MM treated mice (**A**). Ex vivo fluorescent photograph of major organs dissected from mice with different treatments (**B**).
Notes: Blank control (a); $HgCl_2$ poisoned (b); 15 mg/kg of C-DMSA@VES-g-CSO/VES-g-CS MM (c); $HgCl_2$ poisoned with C-DMSA treatment (d); $HgCl_2$ poisoned with 15 mg/kg of C-DMSA@VES-g-CSO/VES-g-CS MM treatment (e); $HgCl_2$ poisoned with 30 mg/kg of C-DMSA@VES-g-CSO/VES-g-CS MM treatment (f).
Abbreviations: IR-775 loaded micelles, vitamin E succinate-grafted-chitosan oligosaccharide/vitamin E succinate-grafted-chitosan mixed micelles.

with Hg^{2+} in kidneys. In contrast, when a poisoned rat administrated with free C-DMSA, low fluorescence in liver but strong fluorescence in kidney was observed (column d in Figure 6B), suggesting fast clearance and reaction of C-DMSA with Hg^{2+} in kidney and low enrichment in liver. These findings were in accordance with the previous biodistribution studies and suggested that the C-DMSA loaded mixed micelles were mostly enriched in liver and therefore particularly suitable for the detection and detoxification of Hg^{2+} ion in liver.

In vivo detoxification in Hg^{2+} poisoned rats

Detoxification effects of C-DMSA@VES-g-CSO/VES-g-CS MM were evaluated by liver coefficients, liver and blood mercury contents before and after treatment and compared with those values from healthy control rats or poisoned rats treated with C-DMSA or saline (Table 2).

Liver coefficients for the Hg^{2+} poisoned group, the free C-DMSA treated group and the two C-DMSA@VES-g-CSO/VES-g-CS MM treated groups (15 and 30 mg/kg) were 5.12%, 4.93%, 4.64% and 4.59%, respectively. Compared with the value of 4.57% in control group, significant reduction and nearly complete recovery of liver coefficients were identified in the mixed micelles-treated groups. In addition, mercury contents in liver and in blood of the two mixed micelles-treated groups were significantly reduced compared with the Hg^{2+} poisoned group and the free C-DMSA treated group ($^*P<0.05$) (Table 2). In particular, after treated with the mixed micelles with the dosage of 30 mg/kg, mercury contents in liver and in blood were reduced from 4.57 μg/g tissue and 0.86 μg/L in the poisoned group down to 2.63 μg/g tissue and 0.52 μg/L, respectively. Moreover, at the same dosage of C-DMSA (15 mg/kg), C-DMSA loaded mixed micelles gave better therapeutic results both in liver coefficient and mercury content in liver and blood than the free C-DMSA. These results indicated a significantly enhanced efficacy of C-DMSA loaded mixed micelles in Hg^{2+} removal in vivo and treatment of Hg^{2+}-induced hepatomegaly compared with the free C-DMSA, which may attribute to the combined effects of elongated circulation time, enhanced cellular uptake and liver-specific delivery of

Table 2 Liver coefficients and contents of total mercury in rat liver and blood

Treatment	Mercury		Liver coefficients (%)
	Liver (μg/g tissue)	Blood (μg/L)	
Control	0.01±0.01	0±0.01	4.57±0.11
$HgCl_2$	4.57±0.42***	0.86±0.18***	5.12±0.11*
$HgCl_2$+C-DMSA (15 mg/kg)	3.64±0.54	0.70±0.19	4.93±0.15
$HgCl_2$+C-DMSA loaded micelles (15 mg/kg)	2.63±0.55#	0.59±0.06#	4.64±0.19#
$HgCl_2$+C-DMSA loaded micelles (30 mg/kg)	2.38±0.29#	0.52±0.02#	4.59±0.13#

Notes: *p<0.05, ***p<0.001, compared to control group. #p<0.05 compared to $HgCl_2$ group. Data were presented as mean±SD (n=6).
Abbreviations: C-DMSA, 3-formyl-7-diethylamino coumarin masked meso-dimercaptosuccinic acid; C-DMSA loaded micelles, C-DMSA loaded vitamin E succinate-grafted-chitosan oligosaccharide/vitamin E succinate-grafted-chitosan mixed micelles.

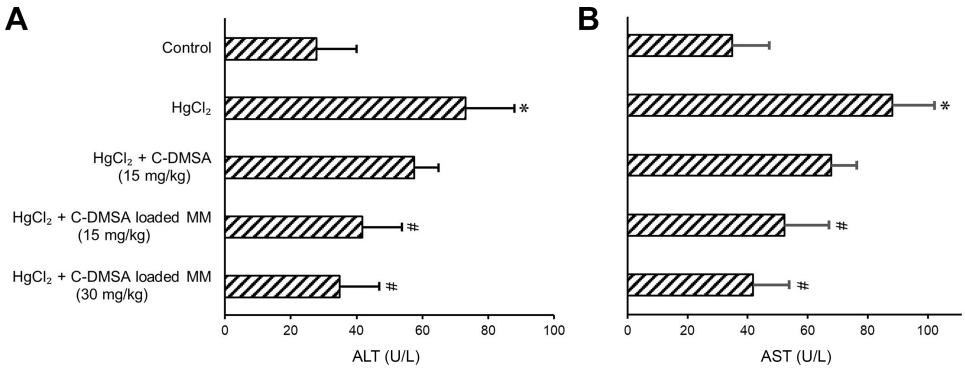

Figure 7 ALT (**A**) and AST (**B**) in blood samples from rats with different treatments.
Notes: *p<0.05, compared to control group; #p<0.05, compared to $HgCl_2$ group. Data were presented as mean±SD (n=6).
Abbreviations: ALT, alanine transaminase; AST, aspartate transaminase; C-DMSA; 3-formyl-7-diethylamino coumarin masked meso-dimercaptosuccinic acid; C-DMSA loaded MM, C-DMSA loaded vitamin E succinate-grafted-chitosan oligosaccharide/vitamin E succinate-grafted-chitosan mixed micelles.

C-DMSA in the formulation of C-DMSA loaded mixed micelles.

To further confirm the detoxification and hepatoprotective effects of C-DMSA loaded mixed micelles, ALT and AST activities in blood were measured (Figure 7A and B), which were biomarkers commonly used for assessment of liver function impairment.[43,44] The results showed that enzyme activities were significantly decreased in the micelles-treated groups compared with the Hg^{2+} poisoned group and the free C-DMSA treated group, strongly supporting that the C-DMSA@VES-g-CSO/VES-g-CS MM were effective in protection of liver cells from Hg^{2+}-induced cell damage.

Conclusion

In the present study, mixed micelles prepared from two polymers were used to load C-DMSA, a theranostic fluorescent probe for Hg^{2+} detection and detoxification, in cell and in vivo applications. The mixed micelles, C-DMSA@VES-g-CSO/VES-g-CS MM showed appealing properties and good stability. In vitro studies showed that the C-DMSA loaded mixed micelles significantly increased C-DMSA cellular uptake and Hg^{2+} detection in L929 cells. Moreover, significantly improved detoxification efficacy was shown in Hg^{2+}-poisoned rat models in terms of mercury contents in blood and in liver. Notably, the C-DMSA loaded mixed micelles showed excellent hepatoprotective activity as evidenced by reduced liver coefficients and reduced ALT and AST activities. Furthermore, ex vivo fluorescence imaging experiments also supported enhanced Hg^{2+} detection in rat liver. The above results suggested that C-DMSA@VES-g-CSO/VES-g-CS MM significantly improved the efficacy of C-DMSA in treatment of mercury poisoning, suggesting the important role of the mixed micelles as a delivery system to increase the cellular uptake of the theranostic probe. More importantly, liver-specific targeting capabilities were achieved by C-DMSA@VES-g-CSO/VES-g-CS MM. To the best of our knowledge, this work provided the first proof of concept studies that a mixed polymeric micelle delivery system could significantly enhance cell uptake and efficacy of a theranostic fluorescent probe for heavy

metal detection and detoxification treatment both in vitro and in vivo. The strategy presented here may provide a promising approach to address the delivery problem of a theranostic probe/drug for diagnosis and treatment of heavy metal poisoning.

Acknowledgment

This work was supported by the National Natural Science Foundation of China (grant no. 21577037, K. L.) , Shanghai Municipal Natural Science Foundation (contract no. 17ZR1406600), Science and Technology Commission of Shanghai Municipality (contract no. 10DZ2220500) and the Shanghai Committee of Science and Technology (grant no. 11DZ2260600).

Disclosure

The authors report no conflicts of interest in this work.

References

1. Ki-Hyun K, Ehsanul K, Shamin AJ. A review on the distribution of Hg in the environment and its human health impacts. *J Hazard Mater*. 2016;306:367–385. doi:10.1016/j.jhazmat.2015.12.006
2. Zhai H, Wang Y, Wang M, et al. Construction of a glutathione-responsive and silica-based nanocomposite for controlled release of chelator dimercaptosuccinic acid. *Int J Mol Sci*. 2018;19(12):3790. doi:10.3390/ijms19123790
3. Cao Y, Skaug MA, Andersen O, et al. Chelation therapy in intoxications with mercury, lead and copper. *J Trace Elem Med Biol*. 2015;31:188–192. doi:10.1016/j.jtemb.2014.04.010
4. Agarwal R, Goel SK, Chandra R, et al. Role of vitamin E in preventing acute mercury toxicity in rat. *Environ Toxicol Pharmacol*. 2010;29:70–78. doi:10.1016/j.etap.2009.10.003
5. Aposhian HV, Morgan DL, Queen HLS, et al. Vitamin C, glutathione, or lipoic acid did not decrease brain or kidney mercury in rats exposed to mercury vapor. *J Toxicol Clin Toxicol*. 2003;41:339–342.
6. Gao Y, Shi Z, Long Z, et al. Determination and speciation of mercury in environmental and biological samples by analytical atomic spectrometry. *Microchem J*. 2012;103:1–14. doi:10.1016/j.microc.2012.02.001
7. Dos Santos JS, de la Guardia M, Pastor A, et al. Determination of organic and inorganic mercury species in water and sediment samples by HPLC on-line coupled with ICP-MS. *Talanta*. 2009;80:207–211. doi:10.1016/j.talanta.2009.06.053
8. Rurack K, Kollmannsberger M, Reschgenger U, et al. A selective and sensitive fluoroionophore for Hg II, Ag I, and Cu II with virtually decoupled fluorophore and receptor units. *J Am Chem Soc*. 2000;122:968–969. doi:10.1021/ja992630a
9. Sakamoto H, Ishikawa J, Nakao S, et al. Excellent mercury (II) ion selectivefluoroionophore based on a 3,6,12,15-tetrathia-9-azaheptadecane derivative-bearing a nitrobenzoxa diazolyl moiety. *Chem Commun*. 2000;23:2395–2396. doi:10.1039/b007577i
10. Liu D, Qu W, Chen W, et al. Highly sensitive, colorimetric detection of mercury(II) in aqueous media by quaternary ammonium group-capped gold nanoparticles at room temperature. *Anal Chem*. 2010;82:9606–9610. doi:10.1021/ac1021503
11. Tan L, Zhang Y, Qiang H, et al. A sensitive Hg(II) colorimetric sensor based on synergistic catalytic effect of gold nanoparticles and Hg. *Sensors Actuat B Chem*. 2016;229:686–691. doi:10.1016/j.snb.2016.02.037
12. Zuo Y, Xu J, Xing H, et al. Simple and green synthesis of piperazine-grafted reduced graphene oxide and its application for the detection of Hg(II). *Nanotechnology*. 2018;29(16):165502. doi:10.1088/1361-6528/aaaf4a
13. Song C, Yang W, Zhou N, et al. Fluorescent theranostic agents for Hg (2+) detection and detoxification treatment. *Chem Commun*. 2015;51:4443–4446. doi:10.1039/c5cc00295h
14. Li L, Wang H, Ong ZY, et al. Polymer and lipid-based nanoparticle therapeutics for the treatment of liver diseases. *Nano Today*. 2010;5:296–312. doi:10.1016/j.nantod.2010.06.007
15. Maximiliano C, Fiorella C, Ezequiel B, et al. Polymeric mixed micelles as nanomedicines: achievements and perspectives. *EurJ Pharm Biopharm*. 2017;113:211–228. doi:10.1016/j.ejpb.2016.12.019
16. Mesquita M, Pedroso TF, Oliveira CS, et al. Effects of zinc against mercury toxicity in female rats 12 and 48 hrs after $HgCl_2$ exposure. *Excli J*. 2016;15:256–267. doi:10.17179/excli2015-709
17. Chen Y, Feng S, Liu W, et al. Vitamin E succinate-grafted-chitosan oligosaccharide/RGD-conjugated TPGS mixed micelles loaded with paclitaxel for U87MG tumor therapy. *Mol Pharm*. 2007;14:1190–1203. doi:10.1021/acs.molpharmaceut.6b01068
18. Lian H, Sun J, Yu Y, et al. Supramolecular micellar nanoaggregates based on a novel chitosan/vitamin E succinate copolymer for paclitaxel selective delivery. *Int J Nanomedicine*. 2011;6:3323–3334. doi:10.2147/IJN.S26305
19. Cagel M, Tesan FC, Bernabeu E, et al. Polymeric mixed micelles as nanomedicines: achievements and perspectives. *Eur J Pharm Biopharm*. 2017;113:211–228. doi:10.1016/j.ejpb.2016.12.019
20. Liu J, Li HX, Chen DQ, et al. In vivo evaluation of novel chitosan graft polymeric micelles for delivery of paclitaxel. *Drug Deliv*. 2011;18(3):181–189. doi:10.3109/10717544.2010.520355
21. Liang N, Sun S, Li X, et al. α-tocopherol succinate-modified chitosan as a micellar delivery system for paclitaxel: preparation, characterization and in vitro/in vivo evaluations. *Int J Pharm*. 2012;423:480–488. doi:10.1016/j.ijpharm.2011.12.004
22. Xie M, Hu B, Wang Y, et al. Grafting of gallic acid onto chitosan enhances antioxidant activities and alters rheological properties of the copolymer. *J Agr Food Chem*. 2014;62:9128–9136. doi:10.1021/jf503207s
23. Aguiar J, Carpena P, Molina-Bolívar JA, et al. On the determination of the critical micelle concentration by the pyrene 1:3 ratio method. *J Colloid Interface Sci*. 2003;258:116–122. doi:10.1016/S0021-9797(02)00082-6
24. Xu Y, Jiang Z, Xiao Y, et al. A new fluorescent turn-on chemodosimeter for mercury ions in solution and its application in cells and organisms. *Anal Chim Acta*. 2014;807:126–134. doi:10.1016/j.aca.2013.11.042
25. Yu SY, Wu SP. A highly selective turn-on fluorescence chemosensor for Hg(II) and its application in living cell imaging. *Sensors Actuat B Chem*. 2014;201:25–30. doi:10.1016/j.snb.2014.04.077
26. Mata R, Nakkala J, Chandra V, et al. In vivo bio-distribution, clearance and toxicity assessment of biogenic silver and gold nanoparticles synthesized from Abutilon indicum in wistar rats. *J Trace Elem Med Biol*. 2018;48:157–165. doi:10.1016/j.jtemb.2018.03.015
27. Bridges CC, Joshee L, Zalups RK. Effect of DMPS and DMSA on the placental and fetal disposition of methylmercury. *Placenta*. 2009;30:800–805. doi:10.1016/j.placenta.2009.06.005
28. Kaur P, Heggland I, Aschner M, et al. Docosahexaenoic acid may act as a neuroprotector for methylmercury-induced neurotoxicity in primary neural cell cultures. *Neurotoxicology*. 2008;29:978–987. doi:10.1016/j.neuro.2008.06.004
29. Tony D, Li X, Bona Y, et al. Phototheranostic nanoplatform based on a single cyanine dye for image-guided combinatorial phototherapy. *Nanomedicine*. 2017;13:955–963. doi:10.1016/j.nano.2016.11.005
30. Rizzetti DA, Torres JGD, Escobar AG, et al. Apocynin prevents vascular effects caused by chronic exposure to low concentrations of mercury. *PLoS One*. 2013;8:e55806. doi:10.1371/journal.pone.0055806

31. Dittert IM, Maranhão TA, Borges DL, et al. Determination of mercury in biological samples by cold vapor atomic absorption spectrometry following cloud point extraction with salt-induced phase separation. *Talanta*. 2007;72:1786–1790. doi:10.1016/j.talanta.2007.02.012
32. Serpe FP, Russo R, Simone AD, et al. Levels of heavy metals in liver and kidney of dogs from urban environment. *Open Vet J*. 2012;2:15–18.
33. Shah AQ, Kazi TG, Baig JA, et al. Total mercury determination in different tissues of broiler chicken by using cloud point extraction and cold vapor atomic absorption spectrometry. *Food Chem Toxicol*. 2010;48:65–69. doi:10.1016/j.fct.2009.09.016
34. Ingrid D, Tatiane M, Daniel B, et al. Determination of mercury in biological samples by cold vapor atomic absorption spectrometry following cloud point extraction with salt-induced phase separation. *Talanta*. 2007;72:1786–1790. doi:10.1016/j.talanta.2007.02.012
35. Choi K-S, Lee CH, ImHong-Joo H-J, et al. Sample pretreatment for the determination of gamma emitting nuclides in dry radioactive waste using a dry ashing and high-performance microwave digestion system. *J Radioanal Nucl Chem*. 2014;301:567–571. doi:10.1007/s10967-014-3163-5
36. Casettari L, Vllasaliu D, Castagnino E, et al. PEGylated chitosan derivatives: synthesis, characterizations and pharmaceutical applications. *Prog Polym Sci*. 2012;37:659–685. doi:10.1016/j.progpolymsci.2011.10.001
37. Huang S, Yu X, Yang L, et al. The efficacy of nimodipine drug delivery using mPEG-PLA micelles and mPEG-PLA/TPGS mixed micelles. *Eur J Pharm Sci*. 2014;63:187–198. doi:10.1016/j.ejps.2014.07.007
38. Wolburg H, Noell S, Fallierbecker P, et al. The disturbed blood-brain barrier in human glioblastoma. *Mol Aspects Med*. 2012;33:579–589. doi:10.1016/j.mam.2012.02.003
39. Li X, You J, Cui F, et al. Preparation and characteristics of stearic acid grafted chitosan oligosaccharide polymeric micelle containing 10-hydroxycamptothecin. *Asian J Pharm Sci*. 2008;3:80–87.
40. Sun L, Chen Y, Zhou Y, et al. Preparation of 5-fluorouracil-loaded chitosan nanoparticles and study of the sustained release in vitro and in vivo. *Asian J Pharm Sci*. 2017;5:418–423. doi:10.1016/j.ajps.2017.04.002
41. Heather G, Dolly H, David W, et al. Nanoparticle uptake: the phagocyte problem. *Nano Today*. 2015;10(4):487–510. doi:10.1016/j.nantod.2015.06.006
42. Klaas P, Jai P, Leonie B. Drug targeting to the diseased liver. *J Control Release*. 2012;161:188–197. doi:10.1016/j.jconrel.2012.02.011
43. Mortazavi SM, Mortazavi G, Paknahad M. A review on the distribution of Hg in the environment and its human health impacts. *J Hazard Mater*. 2016;306:376–385. doi:10.1016/j.jhazmat.2015.11.031
44. Samipillai SS, Elangomathavan R, Ramesh S, et al. Effect of taurine and glutathione on mercury toxity in liver tissue of rats. *Recent Res Sci Technol*. 2009;1:243–249.

Supplementary materials

Determination of critical micelle concentrations

Critical micelle concentrations (CMC) of the VES-g-CSO, VES-g-CS, VES-g-CSO/VES-g-CS (w/w=8:2) were determined on a Lumina fluorescence spectrometer (Thermo Fisher Scientific, Waltham, MA, USA). Solutions containing of 4.94×10^{-7} mol/L pyrene and increasing concentrations (1.0×10^{-4} −1.0 mg/mL) of the polymer to be tested were prepared. Each solution sample was sonicated for 5 mins at 100 W with the pulse turned off for 1 s at intervals of 1 s, incubated at room temperature for 12 hrs in light-resistance containers before its fluorescence emission spectrum was recorded at excitation wavelength 335 nm. CMC values were determined from plots of the intensity ratio of I_1 (373 nm)/I_3 (385 nm) against logarithm of polymer concentrations (Figure S1).

Cytotoxicity study

In vitro cytotoxicity of C-DMSA@VES-g-CSO/VES-g-CS MM was studied on L929 cells by the MTT assay. Cells were seeded at a density of 1×10^4 cells/well in a 96-well plate. After 24-hr incubation, the growth medium was replaced with 200 μL of medium containing different concentrations of free C-DMSA (1–100 μg/mL), VES-g-CSO/VES-g-CS MM (0.01–1 mg/mL) or C-DMSA@VES-g-CSO/VES-g-CS MM (containing 1–100 μg/mL C-DMSA). After incubation for additional 24 hrs in the dark, the drug-containing medium was replaced with PBS and the samples were incubated in a humidified incubator at 37°C with 5% CO_2. PBS was then replaced with fresh medium and MTT solution (500 μg/mL, 200 μL/well) was added, after that the cells were cultured again for 4 hrs. The supernatant was removed, dimethylsulfoxide (200 μL/well) was added and the samples were shaken for 10 mins. The absorbance of each well was measured at 570 nm by a microplate reader (Tecan Safire2, Männedorf, Switzerland) (Figure S2).

Pharmacokinetic profiles

Six male SD rats weighing 170–190 g were randomly divided into two groups for pharmacokinetics studies. Before administration, the rats were fasted for 12 hrs with access to drinking water. Free C-DMSA and C-DMSA@VES-g-CSO/VES-g-CS MM were intravenously injected at an equivalent dose of 10 mg/kg. Blood (0.2 mL) was taken from the orbital venous plexus prior to administration of test substances (0 hr) and after 0.1, 0.25, 0.5, 1, 2, 4, 7, 10 and 24 hrs (n=3 for each time point). The concentration of C-DMSA in the blood samples was determined by a fluorescence spectrophotometer (λ_{Ex} 403 nm and λ_{Em} 480 nm). The related pharmacokinetic parameters were calculated using Kinetic 5.0 software.

The Phase I half-life ($t_{1/2\alpha}$) for C-DMSA and C-DMSA@VES-g-CSO/VES-g-CS MM was calculated at 0.12±0.01 and 0.74±0.12 hrs, respectively, Phase II values ($t_{1/2\beta}$) were 1.91±0.20 and 15.23±1.20 hrs, respectively. Furthermore, the $AUC_{0-24\ hrs}$ for the drug-loaded micelles was 4.57 folds increased compared to free C-DMSA (Table S2). The results demonstrated that the entrapment of C-DMSA in nano drug delivery systems can prolong its circulation.

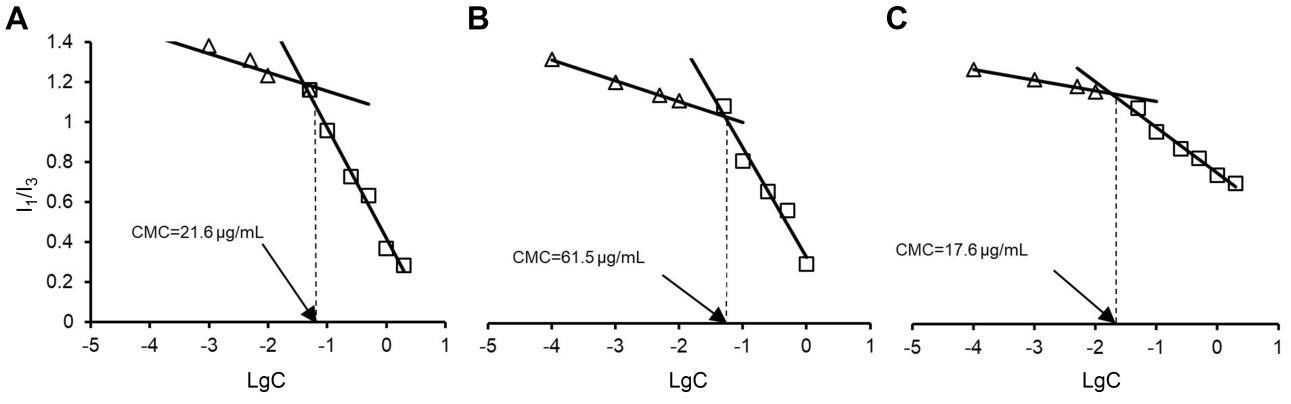

Figure S1 ^{1}H-NMR CS (**A**) and VES (**B**).
Abbreviations: VES, vitamin E succinate; CS, chitosan.

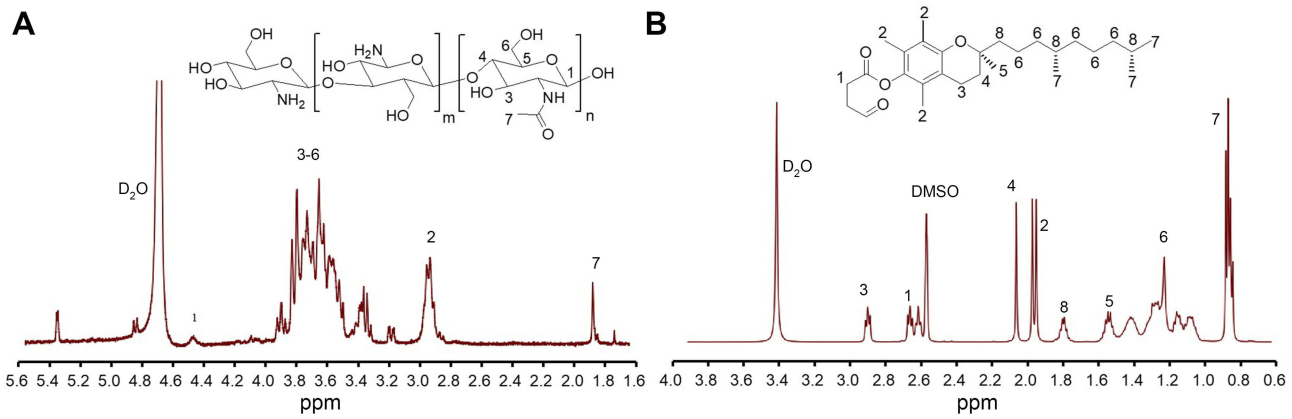

Figure S2 Determination of CMC values of VES-g-CSO/VES-g-CS (w/w=4:1) (**A**), VES-g-CSO (**B**) and VES-g-CS (**C**) solutions.
Abbreviations: CMC, critical micelle concentration; VES-g-CSO, vitamin E succinate-grafted-chitosan oligosaccharide; VES-g-CS, vitamin E succinate-grafted-chitosan; VES-g-CSO/VES-g-CS, vitamin E succinate-grafted-chitosan oligosaccharide/vitamin E succinate-grafted-chitosan.

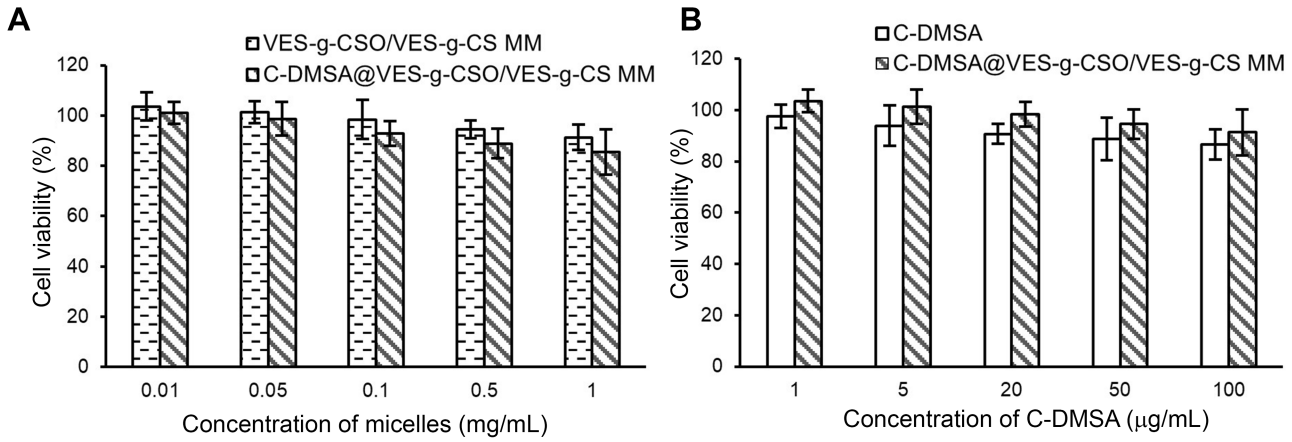

Figure S3 Cell viability of L929 cells treated with the blank mixed micelles (VES-g-CSO/VES-g-CS MM) or C-DMSA@VES-g-CSO/VES-g-CS MM (**A**). Cell viability of L929 cells treated with C-DMSA or C-DMSA@VES-g-CSO/VES-g-CS MM (**B**).
Note: Data were presented as mean±SD (n=3).
Abbreviations: C-DMSA, 3-formyl-7-diethylamino coumarin masked meso-dimercaptosuccinic acid; VES-g-CSO/VES-g-CS MM, vitamin E succinate-grafted-chitosan oligosaccharide/vitamin E succinate-grafted-chitosan mixed micelles; C-DMSA@VES-g-CSO/VES-g-CS MM, C-DMSA loaded vitamin E succinate-grafted-chitosan oligosaccharide/vitamin E succinate-grafted-chitosan mixed micelles.

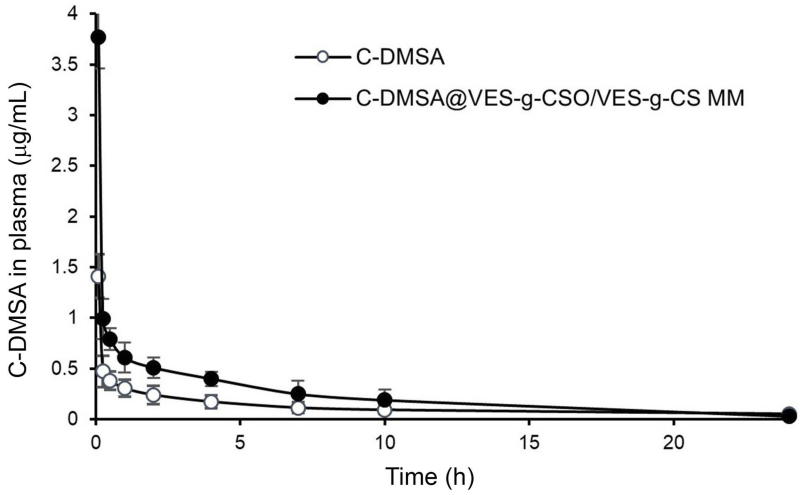

Figure S4 Mean plasma concentration-time curves of C-DMSA after intravenous administration of C-DMSA and C-DMSA@VES-g-CSO/VES-g-CS MM in rats.
Notes: All the rats were received the single dosage at an equivalent dose of 10 mg/kg C-DMSA. Data were presented as mean±SD (n=3).
Abbreviations: C-DMSA, 3-formyl-7-diethylamino coumarin masked meso-dimercaptosuccinic acid; C-DMSA@VES-g-CSO/VES-g-CS MM, C-DMSA loaded vitamin E succinate-grafted-chitosan oligosaccharide/vitamin E succinate-grafted-chitosan mixed micelles.

Table S1 Elemental analysis of VES-g-CSO and VES-g-CS

Polymer	N%	C%	H%	DS (%)
CSO	6.4±0.1	34.1±0.2	6.6±0.1	/
VES-g-CSO	4.5±0.2	34.5±0.2	6.8±0.1	1.2±0.3
CS	7.3±0.0	40.1±0.1	7.2±0.1	/
VES-g-CS	6.4±0.1	40.3±0.8	7.1±0.1	3.0±0.8

Notes: Data were presented as mean ± SD (n=3). "/"means the data is indeterminable.
Abbreviations: DS (%), degree of substitution of VES to amino group of CSO or CS was calculated by elemental analysis; CS, chitosan; CSO, chitosan oligosaccharide; VES-g-CSO, vitamin E succinate- grafted-chitosan oligosaccharide; VES-g-CS, vitamin E succinate-grafted-chitosan.

Table S2 Pharmacokinetic parameters of C-DMSA after a single dosage intravenous administration to rats

Pharmacokinetic parameters	C-DMSA	C-DMSA@VES-g-CSO/VES-g-CS MM
$t_{1/2\alpha}$ (h)	0.12±0.01	0.74±0.12**
$t_{1/2\beta}$ (h)	1.91±0.20	15.23±1.20**
V_d (L/kg)	0.21±0.06	0.17±0.04
$AUC_{0\text{-}24h}$ (μg h/L)	9.96±0.26	45.59±1.37***
CL (L/h/kg)	0.49±0.07	0.10±0.02**

Notes: All the rats were received the single dosage at an equivalent dose of C-DMSA (10 mg/kg). **p<0.01, ***p<0.001, compared to C-DMSA group. Data were presented as mean±SD (n=3).
Abbreviations: $t_{1/2\alpha}$, a rapid distribution half-life; $t_{1/2\beta}$, elimination half-life; AUC, the area under the concentration-time curve; V_d, the apparent volume of the central chamber; CL, clearance; C-DMSA, 3-formyl-7-diethylamino coumarin masked meso-dimercaptosuccinic acid; C-DMSA@VES-g-CSO/VES-g-CS MM, C-DMSA loaded vitamin E succinate-grafted-chitosan oligosaccharide/vitamin E succinate-grafted-chitosan mixed micelles.